

Lyapunov Neural ODE State-Feedback Control Policies

Joshua Hang Sai Ip, Georgios Makrygiorgos, Ali Mesbah

Abstract—Deep neural networks are increasingly used as an effective way to represent control policies in various learning-based control paradigms. For continuous-time optimal control problems (OCPs), which are central to many decision-making tasks, control policy learning can be cast as a neural ordinary differential equation (NODE) problem wherein state and control constraints are naturally accommodated. This paper presents a NODE approach to solving continuous-time OCPs for the case of stabilizing a known constrained nonlinear system around an equilibrium state. The approach, termed Lyapunov-NODE control (L-NODEC), uses a novel Lyapunov loss formulation that incorporates an exponentially-stabilizing control Lyapunov function to learn a state-feedback neural control policy. The proposed Lyapunov loss allows L-NODEC to guarantee exponential stability of the controlled system, as well as its adversarial robustness to perturbations to the initial state. The performance of L-NODEC is illustrated in two problems, including a dose delivery problem in plasma medicine, wherein L-NODEC effectively stabilizes the controlled system around the equilibrium state despite perturbations to the initial state and reduces the inference time necessary to reach equilibrium.

Index Terms—Optimal control, Neural ordinary differential equations, Control Lyapunov function, Robustness.

I. INTRODUCTION

Optimal control is foundational to decision-making for complex dynamical systems [1]–[3]. Efficient solution methods for optimal control problems (OCPs) are essential for tasks such as optimization-based parameter and state estimation, optimal experimental design, and model-based control [4]. Solving continuous-time OCPs is challenging, especially for systems with nonlinear dynamics and path constraints, since these OCPs involve infinitely many decision variables in the form of time-varying functions. Various techniques are developed to solve continuous-time OCPs, including direct methods that approximate the original infinite-dimensional problem as a finite-dimensional one via discretization of the time-varying functions, [5], [6], though discretization can yield a large number of decision variables. Alternatively, indirect methods look to solve the necessary optimality conditions using Pontryagin’s maximum principle or the Hamilton–Jacobi–Bellman equation [7], [8], but may lack scalability to higher-dimensional problems. There are also global optimization methods (e.g., [9], [10]), which fall beyond the scope of this work.

The authors are with the Department of Chemical and Biomolecular Engineering, University of California, Berkeley, CA 94720, USA. {ipjoshua, gmakr, mesbah}@berkeley.edu

This work was supported by the National Science Foundation under Grant 2130734.

In this paper, we adopt a learning perspective to solving continuous-time OCPs. In particular, (deep) neural networks (NN) are widely used to represent control policies in reinforcement learning (RL) for Markov decision processes [11], which fundamentally relies on approximately solving an optimal control problem [12]. Additionally, NN control policies have recently received increasing attention in so-called differentiable control (e.g., [13], [14]) and imitation learning for predictive control (e.g., [15], [16]). The interest in NN control policies stems from their scalability for high-dimensional problems and representation capacity due to universal approximation theorem [17]. However, learning NN policies can be sample inefficient, which is especially a challenge in applications where the policy must be learned via interactions with a real system. On the other hand, when a system model is available in the form of differential equations, the model can be used to formulate a continuous-time OCP while a NN policy is utilized to parameterize the time-varying function of decisions as a state-feedback control policy [18]. This allows for approximating the otherwise intractable OCP, while naturally incorporating path and terminal state constraints into an OCP; what remains a largely open problem in RL.

The latter approach to solving continuous-time OCPs with a NN control policy follows the same strategy as learning neural ordinary differential equations (NODEs) [19]. NODEs comprise a class of NN models that replace the discrete hidden layers in dense NNs with a parameterized ODE that represents continuous-depth models, effectively describing temporal evolution of the hidden states in dynamic inference. Such an interpretation of dynamical systems as a learnable function class offers distinct benefits for time-series modeling (e.g., [20], [21]). In solving continuous-time OCPs, system dynamics can be viewed as a composition of a known ODE model and a NN control policy embedded in the dynamics, forming a NODE structure. This setting is an instance of the universal differential equation framework [22], which embodies the idea of using various types of NNs within physics-based models.

The advantages of *neural* control policies resulting from the NODE approach over traditional NN policies include: (i) allowing the use of modern numerical ODE solvers that leverage adaptive step sizes based on desired accuracy and speed while ensuring numerical stability, which is essential for inference of stiff systems; (ii) handling states and inputs over arbitrary (sampling) time intervals, alleviating the need to discretize data on fixed time intervals as in traditional NNs; and (iii) memory efficiency of NODEs due to the use of the adjoint method [23] for gradient computations in the backward

pass, circumventing backpropagation through the numerical solver. This eliminates the need to store intermediate values in the forward pass, reducing the memory footprint in training neural control policies. Another advantage of using NODEs for control lies in the ability to perform system identification and control policy design in a unified framework [24], [25], enabling performance-oriented model learning [26], [27].

The dynamic nature of NODEs naturally lends itself to leveraging control-theoretic tools to provide desirable structures such as stability in learning neural control policies for OCPs. Stability is particularly crucial in optimal control for establishing robustness properties of the optimal solution to ensure the controlled system reaches its desired state despite perturbations [28]. NN-based control Lyapunov functions (CLFs) have received increasing attention for closed-loop stability analysis (e.g., [29]–[31]). Unlike these approaches, [32] proposed a method for unconstrained autonomous systems to learn NODEs based on the concept of exponentially-stabilizing CLFs [33]. The main idea of this method is to use the supervised loss of NODE as a potential function, so that the NODE training loss embeds both the learnable dynamics and the potential function. Inspired by this notion, we present a new approach to solving continuous-time OCPs, termed Lyapunov-NODE control (L-NODEC), for constrained nonlinear systems with known dynamics. L-NODEC seeks to learn a state-feedback neural control policy that stabilizes the system around a desired equilibrium state. To this end, a novel Lyapunov loss formulation is presented that embeds an exponentially-stabilizing CLF to guarantee exponential stability of the controlled system. Additionally, we prove that L-NODEC guarantees adversarial robustness to uncertain initial conditions by deriving an upper bound on the deviation of the terminal state from the equilibrium state. The superior performance of L-NODEC over NODEC with no stability guarantees is demonstrated using two simulation case studies, including an OCP application in plasma medicine [34].

II. PRELIMINARIES

A. Problem Formulation

For notation convenience without loss of generality, we assume time evolves in the interval $t \in [0, 1]$. Accordingly, we consider the continuous-time OCP

$$\min_{\theta} \int_0^1 \ell(x(t), u(t)) dt + \phi(x(1)), \quad (1a)$$

$$\text{s.t. } \dot{x}(t) = \mathcal{F}(x(t), u(t), t), \quad x(0) = x_0, \quad (1b)$$

$$g(x(t), u(t)) \leq 0, \quad (1c)$$

$$u(t) = \pi_{\theta}(x) \in [u^{lb}, u^{ub}], \quad (1d)$$

where $x \in \mathbb{R}^{n_x}$ is the state with the initial condition x_0 ; $u \in \mathbb{R}^{n_u}$ is the control input constrained within the interval $[u^{lb}, u^{ub}]$, where u^{lb}, u^{ub} are the lower and upper bounds of u , respectively; $\mathcal{F} : \mathbb{R}^{n_x} \times \mathbb{R}^{n_u} \times \mathbb{R} \rightarrow \mathbb{R}^{n_x}$ denotes the system dynamics and is assumed to be affine with respect to u such that $\mathcal{F}(x, t) = f(x, t) + h(x, t)u$, where f, h are known functions; $g : \mathbb{R}^{n_x} \times \mathbb{R}^{n_u} \rightarrow \mathbb{R}$ denotes system constraints; and $\pi_{\theta}(x) : \mathbb{R}^{n_x} \rightarrow \mathbb{R}^{n_u}$ is a static state-feedback control policy parameterized by $\theta \in \mathbb{R}^{n_{\theta}}$. Here, we consider stage and terminal

tracking costs as: $\ell(x(t), u(t)) = (x(t) - x^*)^{\top} P_{\ell} (x(t) - x^*)$ and $\phi(x(1)) = (x(1) - x^*)^{\top} P_{\phi} (x(1) - x^*)$, where $x^* \in \mathbb{R}^{n_x}$ is the equilibrium state and P_{ℓ}, P_{ϕ} are positive definite matrices. The goal is to design a state-feedback control policy $\pi_{\theta}(x)$ that ensures the controlled system is exponentially stable to the equilibrium state x^* and is robust to perturbations in the initial condition x_0 .

B. Neural Ordinary Differential Equations

NODEs provide a useful framework for learning ODEs of the form (1b). In this work, we define NODEs $\mathcal{F}_{\theta}(x, t)$ as

$$\frac{dx}{dt} = \mathcal{F}_{\theta}(x, t) := f(x, t) + h(x, t)\pi_{\theta}(x). \quad (2)$$

NODEs are related to the well-known ResNet [35]. The hidden layers in a ResNet architecture can be viewed as discrete-time Euler’s integration of (2); that is, ResNet can be thought of as learning discrete-time dynamics with a fixed time step. Given θ , (2) can be numerically integrated over a desired time interval for inference of system dynamics. Backpropagation for learning NODEs can be efficiently implemented via the adjoint method [23]. The procedure involves solving a “backward-in-time” ODE associated with (2), known as the adjoint ODE. Solving the adjoint ODE yields gradients of the loss function with respect to states x at each time step. These gradients can then be utilized to calculate the loss function gradients with respect to the learnable parameters θ using the chain rule [19].

The NODE framework enables the use of numerical ODE solvers with adaptive time-steps, which is especially useful for inference of stiff system dynamics. Additionally, the ODE solver embedded in NODEs allows for systematic error growth control and trading off numerical accuracy with efficiency. Despite these advantages, the standard NODE framework does not impose desired structures, such as stability or robustness, within the learned dynamics $\mathcal{F}_{\theta}(x, t)$. In particular, lack of stability in NODEs can lead to fragile solutions to (2).

C. Lyapunov Stability

This work aims to enforce the stability in learning (2). Lyapunov theory generalizes the notion of stability of dynamical systems by reasoning about the convergence of a system to states that minimize a potential function [36]. Potential functions are a special case of dynamic projection.

Definition 1 (Dynamic projection [37]). A continuously differentiable function $V : \mathcal{X} \rightarrow \mathbb{R}$ is a dynamic projection if there exist an $x^* \in \mathcal{X}$ and constants $\underline{\sigma}, \bar{\sigma} > 0$ that satisfy¹

$$\forall x \in \mathcal{X} : \underline{\sigma} \|x - x^*\|_2^2 \leq V(x) \leq \bar{\sigma} \|x - x^*\|_2^2. \quad (3)$$

The notion of dynamic projection can be used to define the exponential stability of (2) as follows.

Definition 2 (Exponential stability). NODEs (2) are exponentially stable if there exist a positive-definite dynamic projection potential function V and a constant $\kappa > 0$ such that all solution trajectories of (2) for all $t \in [0, 1]$ satisfy

$$V(x(t)) \leq V(x(0))e^{-\kappa t}. \quad (4)$$

¹Definition 1 holds for any norm, but l_2 norm is adopted for defining dynamic projection in this work.

We use an exponentially stabilizing control Lyapunov function (ES-CLF) to guarantee the exponential stability of (2).

Theorem 1 (Exponentially stabilizing control Lyapunov function [33]). *For NODEs (2), a locally continuously differentiable positive-definite dynamic projection potential function V is an ES-CLF for all states $x \in \mathcal{X}$ if there exist $\kappa > 0$ and a locally Lipschitz continuous policy $\pi_\theta(x)$ that satisfy*

$$\inf_{\theta \in \Theta} \left[\frac{\partial V}{\partial x} \Big|_x \mathcal{F}_\theta(x, t) + \kappa V(x) \right] \leq 0, \quad \forall t \in [0, 1]. \quad (5)$$

According to (5), there exists $\bar{\theta} \in \Theta$ such that

$$\frac{\partial V}{\partial x} \Big|_x \mathcal{F}_{\bar{\theta}}(x, t) + \kappa V(x) \leq 0, \quad (6)$$

which implies (2) parameterized by $\bar{\theta}$ is exponentially stable with respect to the potential function V .

Inequality (6) enforces a contraction condition on V with respect to time, termed local invariance, meaning this condition holds for local state x instead of the entire trajectory [32]. Next, we will use the NODE framework to learn the state-feedback control policy $\pi_\theta(x)$ in the OCP (1) while imposing the ES-CLF structure as specified in (6). The resulting state-feedback neural control policy will be guaranteed to be exponentially stable with respect to the potential function V .

III. LYAPUNOV-NODE CONTROL (L-NODEC)

We now present the L-NODEC strategy for learning the state-feedback neural control policy $\pi_\theta(x)$ in (1). Given NODEs (2), the continuous-time evolution of states of the controlled system is described by

$$x(t) = x(0) + \int_0^t \mathcal{F}_\theta(x(\tau), \tau) d\tau, \quad \forall t \in [0, 1]. \quad (7)$$

To learn $\pi_\theta(x)$, we must define a loss function. This entails defining a potential function, a pointwise Lyapunov loss, and a Lyapunov loss, as discussed below.

For system (7), we define the potential function as

$$V(x(t)) = (x(t) - x^*)^\top P(x(t) - x^*), \quad (8)$$

where P is a positive definite matrix. The potential function (8) penalizes deviations of $x(t)$ from x^* to effectively steer the system to desired equilibrium x^* .

Theorem 2 (Potential function as a dynamic projection). *The potential function $V(x(t))$ in (8) is a dynamic projection.*

Proof: $V(x(t))$ is a dynamic projection if

$$\underline{\sigma} \|x(t) - x^*\|_2^2 \leq V(x(t)) \leq \bar{\sigma} \|x(t) - x^*\|_2^2. \quad (9)$$

Since P in (8) is a positive definite matrix, there exist constants $\lambda_{min}, \lambda_{max} > 0$ that, respectively, correspond to the smallest and largest eigenvalues of P . Hence, we have

$$\begin{aligned} \lambda_{min} \|x(t) - x^*\|_2^2 &\leq (x(t) - x^*)^\top P(x(t) - x^*) \\ &\leq \lambda_{max} \|x(t) - x^*\|_2^2, \end{aligned} \quad (10)$$

implying $V(x(t))$ is a dynamic projection per Definition 1. ■ By establishing the potential function (8) as a dynamic projection through Theorem 2, we can now utilize (6) to define

a pointwise Lyapunov loss $\mathcal{V}(x(t))$ with respect to the states of the controlled system (7). The pointwise Lyapunov loss is defined as violation of the local invariance for the dynamic projection $V(x(t))$. That is,

$$\mathcal{V}(x(t)) = \max \left\{ 0, \frac{\partial V}{\partial x} \Big|_x \mathcal{F}_\theta(x, t) + \kappa V(x(t)) \right\}. \quad (11)$$

Note that the pointwise Lyapunov loss will take on a non-zero value when it violates the local invariance. To derive the Lyapunov loss, we integrate the pointwise Lyapunov loss (11)

$$\mathcal{L}(\theta) = \int_0^1 \mathcal{V}(x(t)) dt. \quad (12)$$

The Lyapunov loss corresponds to the violation of the local invariance for the entire time domain. The proposed L-NODEC strategy uses the Lyapunov loss (12) to learn the state-feedback neural control policy π_θ so that the learned policy is guaranteed to yield exponentially stable state trajectories for the controlled system (7). The justification for using the Lyapunov loss (12) for learning π_θ stems from the underlying structure of (11), which enforces $\mathcal{V} \geq 0$. This is equivalent to satisfying (6) according to Theorem 1 because the system is penalized with non-negative loss when V is not an ES-CLF.

Theorem 3 (Exponential stability of L-NODEC). *If there exists θ^* such that $\mathcal{L}(\theta^*) = 0$ for a given initial state $x(0)$, then the potential function V in (8) is an ES-CLF according to (6). Thus, the controlled system (7) with the state-feedback neural control policy $\pi_{\theta^*}(x)$ will be exponentially stable.*

Proof: Recall that the Lyapunov loss (12) integrates the pointwise Lyapunov loss (11) over a bounded time domain $t \in [0, 1]$ and (11) satisfies the following conditions: (i) $\mathcal{V}(x) \geq 0$ for all x and t ; and (ii) $\mathcal{V}(x)$ is continuous since it is defined as the maximum of 0 and a differentiable function. We proceed via contradiction. Suppose $\mathcal{V}(x) > 0$. According to (12), the integral will evaluate a strictly positive value, which would then violate the requirement that $\mathcal{L}(\theta^*) = 0$. Hence, $\mathcal{L}(\theta^*) = 0$ implies $\mathcal{V}(x) = 0$ for all x on $t \in [0, 1]$. According to Theorem 1, $\mathcal{V}(x) = 0$ necessitates (6), which indicates that the potential function V is an ES-CLF. This will directly lead to exponential stability of (7) with $\pi_{\theta^*}(x)$. ■

Furthermore, L-NODEC yields neural control policies that are adversarially robust to perturbations in the initial state $x(0)$. This property arises from the pointwise Lyapunov loss (11) with the local invariance since exponential stability will steer the states to an equilibrium state x^* . To analyze adversarial robustness, we must first define stable inference dynamics.

Definition 3 (δ -Stable inference dynamics for $(x(0), x^*)$ [32]). For system (7) with the optimal neural control policy $\pi_{\theta^*}(x)$ and potential function $V(x(t))$ in (8), the initial state-equilibrium pair $(x(0), x^*)$ has δ -stable inference dynamics for $\delta > 0$ if it satisfies:

- 1) Exponential stability: The potential function $V(x(t))$ fulfills (6);
- 2) δ -final loss: The potential function at the final time $t = 1$ satisfies $V(x(1)) \leq V(x(0))e^{-\kappa} \leq \delta$ for $\kappa > 0$.

Definition 3 states that the controlled system (7) with the optimal policy is not only exponentially stable, but also its

potential function at the final inference time $t = 1$ is bounded by a constant δ . Thus, the potential function (8) associated with the optimal trajectories will be an ES-CLF with δ -stable inference dynamics. We now establish an upper bound for δ when the initial state is subject to perturbations.

Theorem 4 (Adversarial robustness of L-NODEC). *For system (7) with the optimal neural control policy $\pi_{\theta^*}(x)$ and the initial state-equilibrium pair $(x(0), x^*)$ that satisfies the conditions of Definition 3, a perturbation ϵ to the initial state $x(0)$, where $\|\epsilon\|_\infty \leq \bar{\epsilon}$ with $\bar{\epsilon}$ being a constant, ensures that δ remains upper bounded as*

$$\delta \leq \lambda_{max} e^{-\kappa} \|x(0) - x^*\|_2^2 - \frac{L\bar{\epsilon}}{\kappa} (1 - e^{-\kappa}), \quad (13)$$

where λ_{max} is the largest eigenvalue of the positive definite matrix P in the potential function (8).

Proof: We begin by taking the derivative of $V(x(t))$

$$\dot{V}(x) = \frac{d}{dt} V(x) = \frac{\partial V}{\partial x} \Big|_x^\top \mathcal{F}_\theta(x, t). \quad (14)$$

Subsequently, we can write

$$\dot{V}(x + \epsilon) \quad (15)$$

$$= \dot{V}(x) + \dot{V}(x + \epsilon) - \dot{V}(x) \quad (16)$$

$$\leq \dot{V}(x) + |\dot{V}(x + \epsilon) - \dot{V}(x)| \quad (17)$$

$$\leq \dot{V}(x) + \left| \frac{\partial V}{\partial x} \Big|_x^\top \mathcal{F}_\theta(x + \epsilon, t) - \frac{\partial V}{\partial x} \Big|_x^\top \mathcal{F}_\theta(x, t) \right| \quad (18)$$

$$\leq \dot{V}(x) + L_V L_f \|\epsilon\|_\infty, \quad (19)$$

where in (19) the global uniform Lipschitz constant for functions V and f is denoted by L_V and L_f , respectively. By defining $L = L_V L_f$ and applying the adversarial perturbation bound $\|\epsilon\|_\infty \leq \bar{\epsilon}$, (19) becomes

$$\dot{V}(x + \epsilon) \leq \dot{V}(x) + L\bar{\epsilon} \quad (20)$$

$$\dot{V}(x + \epsilon) \leq -\kappa V(x) + L\bar{\epsilon}. \quad (21)$$

In (21), Theorem 1 is invoked to rewrite the inequality based on the exponential stability property. We now consider a dynamical system with the upper bound of (21), i.e.,

$$\dot{\gamma} = -\kappa\gamma(t) + L\bar{\epsilon}. \quad (22)$$

Since (22) is a linear ODE, it can be solved for γ as

$$\gamma(t) = e^{-\kappa t} c + \frac{L\bar{\epsilon}}{\kappa}, \quad (23)$$

where c is a constant. Given $\gamma(0)$, (23) can be rewritten as

$$\gamma(t) = e^{-\kappa t} \gamma(0) + \frac{L\bar{\epsilon}}{\kappa} (1 - e^{-\kappa t}). \quad (24)$$

To use the Comparison Lemma [38], we specify $\gamma(0)$ such that $V(x(0)) \leq \gamma(0)$. Recall the second condition of Definition 3, i.e., $V(x(0)) \leq \delta e^\kappa$. By choosing $\gamma(0) = \delta e^\kappa$, (24) becomes

$$\gamma(t) = \delta e^{\kappa(1-t)} + \frac{L\bar{\epsilon}}{\kappa} (1 - e^{-\kappa t}). \quad (25)$$

The conditions to satisfy the Comparison Lemma are met as:

- 1) $\dot{V}(x)$ and $\dot{\gamma}(t)$ are both continuous in state and time;
- 2) $\dot{V}(x) \leq \dot{\gamma}(t)$ for $t \in [0, 1]$;
- 3) $V(x(0)) \leq \gamma(0)$.

Therefore, it can be concluded that $V(x) \leq \gamma(t)$. Recall Theorem 2 where an upper bound on $V(x)$ is derived as

$$V(x) \leq \lambda_{max} \|x(t) - x^*\|_2^2. \quad (26)$$

With exponential stability as stated in Definition 2, the potential function can be upper bounded by the result from (26)

$$V(x) \leq V(x(0)) e^{-\kappa t} \leq \lambda_{max} e^{-\kappa t} \|x(0) - x^*\|_2^2. \quad (27)$$

Based on (27), it suffices to show $\gamma(t) \leq \lambda_{max} e^{-\kappa t} \|x(0) - x^*\|_2^2$. To derive the upper bound on δ , we evaluate the latter inequality, along with (25), at $t = 1$, which yields

$$\delta \leq \lambda_{max} e^{-\kappa} \|x(0) - x^*\|_2^2 - \frac{L\bar{\epsilon}}{\kappa} (1 - e^{-\kappa}). \quad (28)$$

The upper bound on δ provides a guarantee of the adversarial robustness of the neural control policy learned via L-NODEC. If the dynamics of the controlled system (7) are exponentially stable, the dynamics will remain exponentially stable with respect to perturbations in the initial state $x(0)$. ■

IV. L-NODEC LEARNING FRAMEWORK

In this section, we discuss how system constraints can be incorporated into the L-NODEC framework, followed by the neural control policy learning algorithm.

A. System constraints

The L-NODEC strategy can be modified to enforce the state and input constraints (1c) and (1d), respectively. The inputs designed by the neural control policy can be constrained in the last layer of the neural policy by using a sigmoid activation function, commonly defined as $\sigma(\cdot): \mathbb{R} \rightarrow [0, 1]$, i.e.,

$$u_i = u_i^{lb} + (u_i^{ub} - u_i^{lb}) \sigma(\cdot), \quad \forall i \in [1, \dots, n_u]. \quad (29)$$

To enforce state constraints (1c), penalty terms in the form of quadratic of the constraint violation [39] are appended to the pointwise Lyapunov loss (11), leading to

$$\mathcal{V}_c(x(t)) = \max \left\{ 0, \frac{\partial V}{\partial x} \Big|_x^\top \mathcal{F}_\theta(x, t) + \kappa V(x(t)) \right\} + \beta \max \{0, g(x, u)\}^2, \quad (30)$$

where β is a penalty parameter. This is a popular approach to enforcing state constraints since the penalty convergence theorem guarantees a feasible solution to the reformulated unconstrained optimization problem, which is equivalent to solving a constrained optimization problem with Karush-Kuhn-Tucker multipliers [40], [41]. However, since (30) is composed of two terms, there exists a tradeoff between exponential stability of the controlled system (7) and satisfaction of the state constraints (1c), as illustrated in Section V. Other methods can also be used to enforce state constraints. Two alternatives include control barrier functions, which are generally suitable for enforcing hard constraints for safety-critical systems, but they can be conservative [42]; and the augmented Lagrangian method, which can be computationally expensive [43]. These approaches can be investigated in future work.

Algorithm 1 The L-NODEC algorithm for learning state-feedback neural control policies for the OCP (1).

inputs

- M number of max iterations of policy learning
- Γ number of time discretization segments in (31)
- α learning rate
- κ exponential stability parameter in (4)
- β penalty parameter for the state constraint in (30)

for $k \leq M$ **do**

for $i \leq \Gamma - 1$ **do**

- compute** potential $V(x(t_i))$ via (8)
- compute** pointwise Lyapunov loss $\mathcal{V}_c(x(t_i))$ via (30)
- compute** $x(t_{i+1})$ with $\pi_\theta(x(t_i))$ via (7)

end for

- compute** discretized Lyapunov loss $\mathcal{L}(\theta)$ via (31)

- update** $\theta \leftarrow \theta - \alpha(d\mathcal{L}(\theta)/d\theta)$ via (34)

end for

return θ

B. Neural control policy learning

To learn the neural control policy $\pi_\theta(x)$, the Lyapunov loss function (12) must be discretized. To this end, the time interval $[0, 1]$ is discretized into Γ uniform segments. This results in the discretized Lyapunov loss

$$\mathcal{L}(\theta) \approx \sum_{i=0}^{\Gamma-1} \mathcal{V}_c(x(t_i)), \quad (31)$$

which can be evaluated in terms of the pointwise Lyapunov loss (11), or the constrained pointwise Lyapunov loss (30).

To learn the policy, instead of directly backpropagating through the dynamics of the controlled system (7) that can be prohibitively expensive, the adjoint sensitivity method [44] is used to backpropagate through the adjoint ODE

$$a(t) = \frac{\partial \mathcal{L}}{\partial x}, \quad (32)$$

$$\frac{da(t)}{dt} = a(t)^\top \frac{\partial \mathcal{F}_\theta(x, t)}{\partial x}, \quad (33)$$

where $a(t)$ is the adjoint variable. Equation (33) is solved backwards using an ODE solver with the initial condition $a(1)$, along with solving (7). This provides the necessary variables to compute the gradient $d\mathcal{L}/d\theta$ for backpropagation [19]

$$\frac{d\mathcal{L}}{d\theta} = - \int_1^0 a(t)^\top \frac{\partial \mathcal{F}_\theta(x, t)}{\partial \theta} dt. \quad (34)$$

The L-NODEC algorithm for learning state-feedback neural control policies for the continuous-time OCP (1) is summarized in Algorithm 1. For a given initial state-equilibrium pair $(x(0), x^*)$, a trajectory of states is generated from iteratively deriving the optimal input and using an ODE solver to determine the next state according to (7). This allows for evaluating the potential function (8), the pointwise Lyapunov loss (30), and the discretized Lyapunov loss (31). The Lyapunov loss is then utilized to update the neural state-feedback control policy π_θ via backpropagation with the adjoint method.

V. CASE STUDIES

The performance of L-NODEC is demonstrated on a benchmark double integrator problem and a cold atmospheric plasma system with prototypical applications in plasma medicine. The performance of L-NODEC is compared to that of neural ODE control (NODEC) [18].²

A. Double integrator problem

The continuous-time OCP is adapted from [45] as

$$\min_{\theta} \int_0^{t_f} (x(t) - x^*)^\top P_\ell (x(t) - x^*) dt \quad (35a)$$

$$\text{s.t. } \dot{x}_1(t) = x_2, \quad (35b)$$

$$\dot{x}_2(t) = u, \quad (35c)$$

$$u(t) = \pi_\theta(x) \in [-10, 10], \quad (35d)$$

$$x_2(t) \leq x_2^{ub}, \quad (35e)$$

where x_1 denotes position (m), x_2 denotes velocity (m/s), $x_2^{ub} = 2.8$ m/s denotes the upper constraint for x_2 , u denotes the input acceleration (m/s²), and $t_f=1.5$ s. The initial state $x(0)$ and the equilibrium state x^* are set to $(0, 0)$ and $(1, 0)$, respectively. We consider two cases: unconstrained L-NODEC wherein the state constraint (35e) is ignored and constrained L-NODEC that solves (35). In both cases, the potential function is defined as in (8) with $P = P_\ell = \begin{bmatrix} 1 & 0 \\ 0 & 1e^{-6} \end{bmatrix}$.³

Fig. 1 shows the phase portrait of state trajectories for unconstrained L-NODEC compared to that of NODEC [18] that does not impose the proposed stability structure in learning π_θ . Trajectories corresponding to perturbations in the initial state $x(0)$ are also displayed. Both NODEC and L-NODEC trajectories reach the equilibrium state with zero velocity, but NODEC trajectories exhibit a larger range of velocities and positions, as well as larger variance due to perturbations to $x(0)$. Both methods yield policies that accelerate the object for increased velocity to cover distance and, subsequently, decelerate the object to zero velocity, as specified in the equilibrium state. However, the NODEC policy leads to a greater peak velocity, which inevitably causes the object to exceed the desired position of 1 m (Fig. 1 left). In contrast, L-NODEC shows a lower peak velocity and mitigates the ‘‘overshooting’’ behavior of NODEC due to its stability structure.

Fig. 2 shows the position trajectories of the double integrator controlled by the neural control policies designed by NODEC, unconstrained L-NODEC, and constrained L-NODEC. L-NODEC enforces stability by reducing the maximum velocity attained by the object, which results in trajectories that do not exceed the equilibrium position of 1 m, unlike NODEC. Exceeding the equilibrium position and then compensating for it is inefficient, i.e., the average acceleration input for the nominal trajectories of NODEC and unconstrained L-NODEC are 4.43 m/s² and 3.26 m/s², respectively. Fig. 2 also suggests

²In both case studies, the neural control policy π_θ is parameterized by 3 hidden layers of 32 nodes each, and the Adam optimizer is used for policy training. The codes are given at <https://github.com/ipjoshua1483/L-NODEC>.

³The hyperparameters in Algorithm 1 are set to $M = 400$, $\Gamma = 500$, $\alpha = 0.025$, $\kappa = 5$, $\beta = 5$.

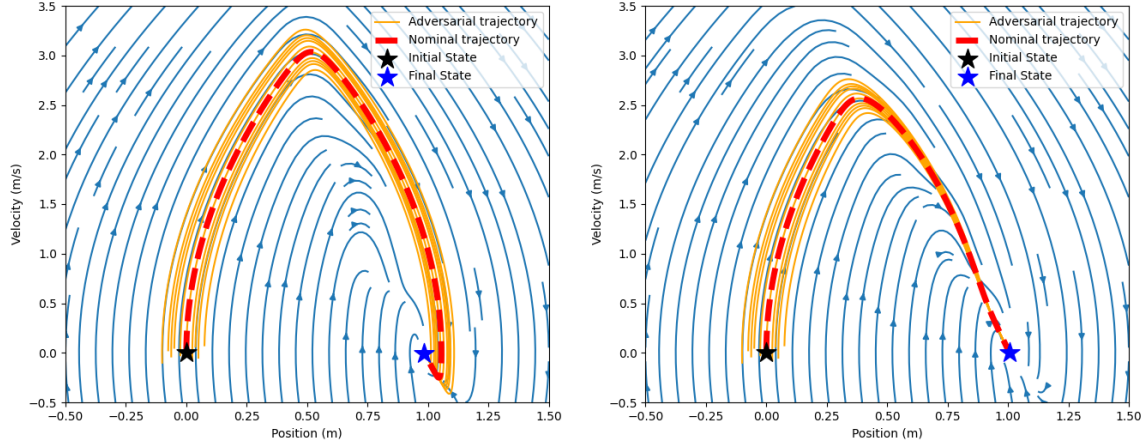


Fig. 1. Phase portraits of the controlled double integrator system. State trajectories for NODEC (left) and L-NODEC (right). The nominal trajectory and adversarial trajectories are shown in red and orange, respectively. The adversarial trajectories are based on different initial states generated around the nominal $x(0) = (0, 0)$ using Sobol points over $[-0.1, 0.1]$. black trajectories signify streamlines in the phase space.

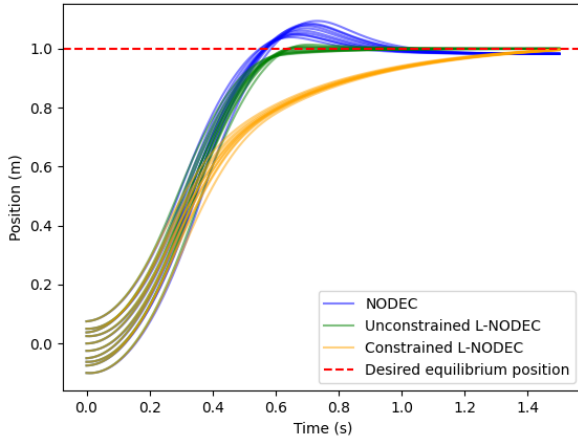


Fig. 2. Position trajectories of the controlled double integrator system for different initial states generated around the nominal $x(0) = (0, 0)$ using Sobol points over $[-0.1, 0.1]$.

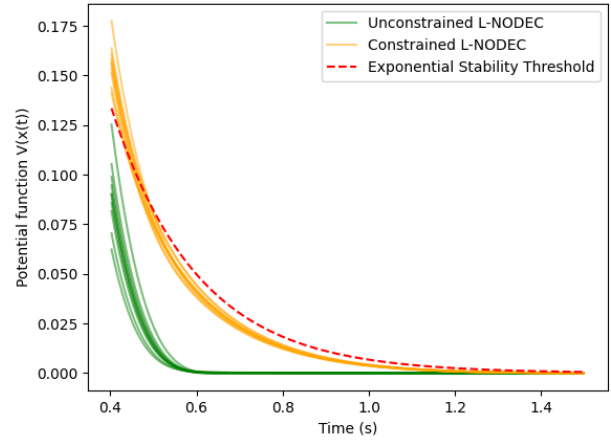


Fig. 3. Normalized potential function for $t \in [0.4, 1.5]$ s.

that constrained L-NODEC requires a longer time to reach the equilibrium position, which is due to the tradeoff between the exponential stability and constraint satisfaction (see (30)). Furthermore, an empirical robustness analysis is performed for NODEC and L-NODEC with 100 Sobol points in the radius of $[-0.1, 0.1]$ around the nominal initial state $x(0) = (0, 0)$. We observed 95% and 0% constraint violations for NODEC and L-NODEC, respectively, highlighting L-NODEC's ability to provide adversarial robustness to perturbations to $x(0)$.

Fig. 3 shows the time-evolution of the potential function $V(x(t))$ for unconstrained and constrained L-NODEC, along with the exponential stability threshold from (4) as a baseline. The neural control policies are capable of steering the system to below the stability threshold over $[0, 1.5]$ s. Constrained L-NODEC gives trajectories that require more time to meet the exponential stability threshold due to the trade-off between

exponential stability and constraint satisfaction.

Fig. 4 shows the estimated domain of attraction (DOA) for NODEC and L-NODEC with the initial state $x(0)$ bounded within $x_1 \in [-0.25, 1.25], x_2 \in [-0.5, 0.5]$. The two DOA are largely similar, suggesting that both methods exhibit comparable performance in reaching the equilibrium state. Generally, initial velocities in the direction of the equilibrium leads to NODEC successfully and L-NODEC unsuccessfully reaching the target state, whereas the opposite is true for initial velocities in the opposite direction. The discrepancy in the two DOA is attributed to how exponential stability is more difficult to establish when the object is moving towards the equilibrium (1, 0) at a sufficiently high velocity initially. The initial velocity in the opposite direction enables exponential stability for L-NODEC, but NODEC struggles because it overcompensates for the lower initial velocity and accelerates the object such that it cannot be steered to the equilibrium.

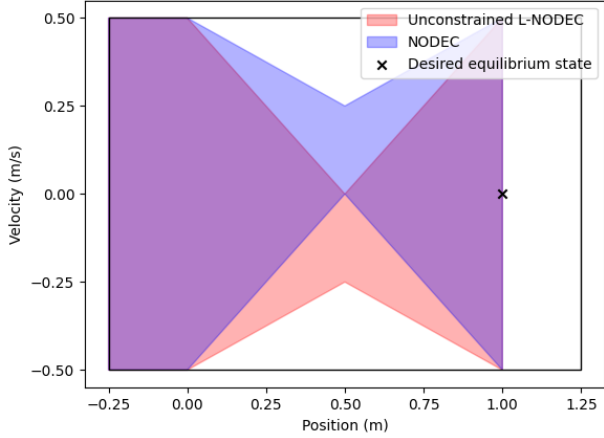


Fig. 4. Estimated domain of attraction for NODEC and L-NODEC. The equilibrium state is displayed with a black cross.

B. Control of thermal dose delivery in plasma medicine

Cold atmospheric plasmas (CAPs) are used for treatment of heat-sensitive biomaterials in plasma medicine [46], [47]. We focus on optimal control of cumulative thermal effects of a biomedical CAP device on a surface. The control objective is to deliver a desired amount of thermal dose, quantified in terms of cumulative equivalent minutes (CEM) [34], to a surface while maintaining the surface temperature below a safety-critical threshold. The OCP is formulated as [48]

$$\min_{\theta} \int_0^{t_f} (x(t) - x^*)^\top P_\ell (x(t) - x^*) dt \quad (36a)$$

$$\text{s.t. } \dot{x}_1(t) = \frac{u}{3.1981} - \frac{0.8088}{\ln(x_1(t) - 25) - \ln(x_1(t) - 35)}, \quad (36b)$$

$$\dot{x}_2(t) = \frac{0.5^{(43-x_1(t))}}{60}, \quad (36c)$$

$$u(t) = \pi_\theta(x) \in [1, 5], \quad (36d)$$

$$x_1(t) \leq x_1^{ub}, \quad (36e)$$

where x_1 denotes the surface temperature ($^\circ\text{C}$) with the threshold $x_1^{ub} = 45^\circ\text{C}$, x_2 denotes the thermal dose CEM (min), the control input u is the power applied to CAP (W), and $t_f = 100$ s. The initial and equilibrium states are $x(0) = (37, 0)$ and $x^* = (37, 1.5)$, respectively. The potential function is defined as in (8) with $P = P_\ell = \begin{bmatrix} 1e^{-10} & 0 \\ 0 & 1e^{-2} \end{bmatrix}^4$.

We compare the performance of L-NODEC to that of NODEC with the stage cost (36a) and NODEC with the terminal cost $(x(t_f) - x^*)^\top P_\phi (x(t_f) - x^*)$ where $P_\phi = P_\ell$. A terminal cost formulation naturally reflects the goal of delivering the desired plasma dose within a prespecified treatment time [47]. Fig. 5 shows the CEM delivered to the target surface, surface temperature, and control input of the applied power for each strategy. 50 adversarial trajectories are generated based on a 5°C perturbation radius around the

⁴The hyperparameters in Algorithm 1 are set to $M = 400$, $\Gamma = 500$, $\alpha = 0.025$, $\kappa = 5$, $\beta = 50$.

nominal initial temperature via Sobol sampling. The state trajectories are truncated when the desired thermal dose of 1.5 min is reached to avoid excessive thermal dose delivery (i.e., plasma treatment is aborted). The average time to reach CEM of 1.5 min is 46 s, 67 s, and 96 s for L-NODEC, NODEC with stage cost, and NODEC with terminal cost, respectively. This is significant in plasma medicine since shorter treatment times are desirable due to patient safety and comfort [47]. Additionally, L-NODEC trajectories exhibit the lowest variance, especially in comparison with NODEC with terminal cost. L-NODEC initially maintains the applied power at a higher level (Fig. 5(c)), which results in higher temperature in the initial phase of the treatment, leading to quicker accumulation of CEM till the temperature constraint is reached. Then, L-NODEC reduces the applied power level once it is close to reaching the target CEM. NODEC maintains a lower level of applied power to gradually accumulate CEM. As for NODEC with terminal cost, the lack of information on the target CEM until the final inference time t_f results in trajectories that take considerably longer to achieve CEM of 1.5 min. This is reflected by the even lower maximum applied power. These results suggest that L-NODEC provides a versatile formulation that aids in reducing the inference time.

VI. CONCLUSION

This paper addressed exponential stability and adversarial robustness of the neural ordinary differential equation approach to solving continuous-time optimal control problems. The numerical illustrations demonstrated the importance of accounting for exponential stability to ensure solution robustness to perturbations in the initial state. Future work will investigate alternative approaches to constraint handling.

REFERENCES

- [1] M. Athans and P. L. Falb, *Optimal control: an introduction to the theory and its applications*. Courier Corporation, 2007.
- [2] F. L. Lewis, D. Vrabie, and V. L. Syrmos, *Optimal control*. John Wiley & Sons, 2012.
- [3] R. Stengel, *Optimal control and estimation*. Courier Corporation, 1994.
- [4] A. E. Bryson, *Applied optimal control: optimization, estimation and control*. Routledge, 2018.
- [5] K.-L. Teo, C.-J. Goh, K.-H. Wong *et al.*, *A unified computational approach to optimal control problems*. Longman Scientific & Technical New York, 1991, vol. 113.
- [6] L. T. Biegler, A. M. Cervantes, and A. Wächter, "Advances in simultaneous strategies for dynamic process optimization," *Chemical Engineering Science*, vol. 57, no. 4, pp. 575–593, 2002.
- [7] R. F. Hartl, S. P. Sethi, and R. G. Vickson, "A survey of the maximum principles for optimal control problems with state constraints," *SIAM Review*, vol. 37, no. 2, pp. 181–218, 1995.
- [8] R. Luus, *Iterative dynamic programming*. Chapman and Hall, 2019.
- [9] B. Chachuat, A. B. Singer, and P. I. Barton, "Global methods for dynamic optimization and mixed-integer dynamic optimization," *Industrial & Engineering Chemistry Research*, vol. 45, pp. 8373–8392, 2006.
- [10] D. Rodrigues and A. Mesbah, "Efficient global solutions to single-input optimal control problems via approximation by sum-of-squares polynomials," *IEEE Transactions on Automatic Control*, vol. 67, no. 9, pp. 4674–4686, 2022.
- [11] R. S. Sutton and A. G. Barto, *Reinforcement Learning: An Introduction*. MIT Press, Cambridge, 2018.
- [12] D. Bertsekas, *Reinforcement learning and optimal control*. Athena Scientific, 2019, vol. 1.

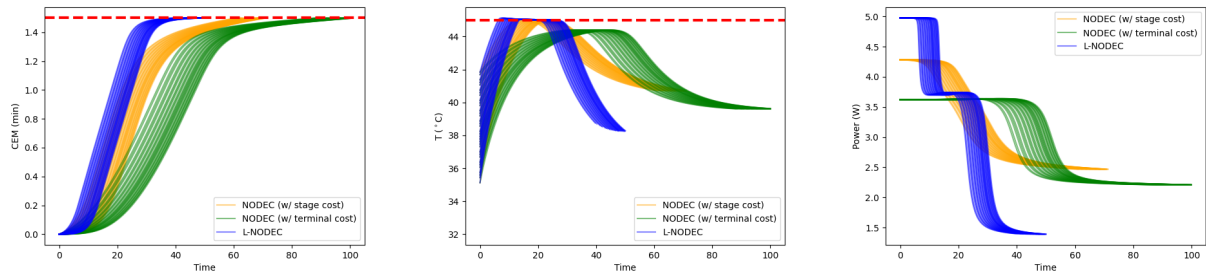


Fig. 5. Optimal control of thermal dose delivery of cold atmospheric plasma to a target surface for NODEC with stage cost, NODEC with terminal cost, and L-NODEC. (a) The delivered thermal dose CEM. (b) Surface temperature. (c) Control input, i.e., applied power to plasma. Adversarial trajectories are generated from a distribution of 50 Sobol points with a perturbation radius of 5°C around the nominal initial temperature.

[13] W. Jin, Z. Wang, Z. Yang, and S. Mou, "Pontryagin differentiable programming: An end-to-end learning and control framework," *Advances in Neural Information Processing Systems*, vol. 33, pp. 7979–7992, 2020.

[14] J. Drgoňa, K. Kiš, A. Tuor, D. Vrabie, and M. Klaučo, "Differentiable predictive control: Deep learning alternative to explicit model predictive control for unknown nonlinear systems," *Journal of Process Control*, vol. 116, pp. 80–92, 2022.

[15] A. Mesbah, K. P. Wabersich, A. P. Schoellig, M. N. Zeilinger, S. Lucia, T. A. Badgwell, and J. A. Paulson, "Fusion of machine learning and MPC under uncertainty: What advances are on the horizon?" in *Proceedings of the American Control Conference*, 2022, pp. 342–357.

[16] J. A. Paulson and A. Mesbah, "Approximate closed-loop robust model predictive control with guaranteed stability and constraint satisfaction," *IEEE Control Systems Letters*, vol. 4, no. 3, pp. 719–724, 2020.

[17] A. R. Barron, "Universal approximation bounds for superpositions of a sigmoidal function," *IEEE Transactions on Information Theory*, vol. 39, no. 3, pp. 930–945, 1993.

[18] I. O. Sandoval, P. Petsagkourakis, and E. A. del Rio-Chanona, "Neural odes as feedback policies for nonlinear optimal control," *IFAC-Papers onLine*, vol. 56, no. 2, pp. 4816–4821, 2023.

[19] R. T. Q. Chen, Y. Rubanova, J. Bettencourt, and D. K. Duvenaud, "Neural ordinary differential equations," *Advances in Neural Information Processing Systems*, vol. 31, 2018.

[20] A. Rahman, J. Drgoňa, A. Tuor, and J. Strube, "Neural ordinary differential equations for nonlinear system identification," in *Proceedings of the American Control Conference*, 2022, pp. 3979–3984.

[21] A. J. Linot, J. W. Burby, Q. Tang, P. Balaprakash, M. D. Graham, and R. Maulik, "Stabilized neural ordinary differential equations for long-time forecasting of dynamical systems," *Journal of Computational Physics*, vol. 474, p. 111838, 2023.

[22] C. Rackauckas, Y. Ma, J. Martensen, C. Warner, K. Zubov, R. Supekar, D. Skinner, A. Ramadhan, and A. Edelman, "Universal differential equations for scientific machine learning," *arXiv:2001.04385*, 2020.

[23] D. Givoli, "A tutorial on the adjoint method for inverse problems," *Computer Methods in Applied Mechanics and Engineering*, vol. 380, p. 113810, 2021.

[24] S. Bachhuber, I. Weygers, and T. Seel, "Neural ODEs for data-driven automatic self-design of finite-time output feedback control for unknown nonlinear dynamics," *IEEE Control Systems Letters*, 2023.

[25] C. Chi, "Nodec: Neural ode for optimal control of unknown dynamical systems," *arXiv preprint arXiv:2401.01836*, 2024.

[26] M. Gevers, "Identification for control: From the early achievements to the revival of experiment design," *European journal of control*, vol. 11, no. 4-5, pp. 335–352, 2005.

[27] G. Makrygiorgos, A. Bonzanini, V. Miller, and A. Mesbah, "Performance-oriented model learning for control via multi-objective Bayesian optimization," *Comput. Chem. Eng.*, vol. 162, p. 107770, 2022.

[28] D. Bertsekas, *Dynamic Programming and Optimal Control*. Athena Scientific, Belmont, 2012, vol. 1.

[29] Y.-C. Chang, N. Roohi, and S. Gao, "Neural Lyapunov control," *Advances in Neural Information Processing Systems*, vol. 32, 2019.

[30] S. Mukherjee, J. Drgoňa, A. Tuor, M. Halappanavar, and D. Vrabie, "Neural Lyapunov differentiable predictive control," in *Proceedings of the 61st IEEE Conference on Decision and Control*, 2022, p. 2097.

[31] L. Zhao, K. Miao, K. Gatsis, and A. Papachristodoulou, "NLBAC: A neural ordinary differential equations-based framework for stable and safe reinforcement learning," *arXiv preprint arXiv:2401.13148*, 2024.

[32] I. D. J. Rodriguez, A. Ames, and Y. Yue, "Lyantet: A lyapunov framework for training neural odes," in *International conference on machine learning*. PMLR, 2022, pp. 18 687–18 703.

[33] A. D. Ames, K. Galloway, K. Sreenath, and J. W. Grizzle, "Rapidly exponentially stabilizing control Lyapunov functions and hybrid zero dynamics," *IEEE Transactions on Automatic Control*, vol. 59, p. 876, 2014.

[34] D. Gidon, D. B. Graves, and A. Mesbah, "Effective dose delivery in atmospheric pressure plasma jets for plasma medicine: A model predictive control approach," *Plasma Sources Science and Technology*, vol. 26, no. 8, p. 085005, 2017.

[35] E. Haber and L. Ruthotto, "Stable architectures for deep neural networks," *Inverse Problems*, vol. 34, no. 1, p. 014004, 2017.

[36] J. L. Salle and S. Lefschetz, *Stability by Liapunov's Direct Method: With Applications*. New York: Academic Press, 1961.

[37] A. J. Taylor, V. D. Dorobantu, M. Krishnamoorthy, H. M. Le, Y. Yue, and A. D. Ames, "A control Lyapunov perspective on episodic learning via projection to state stability," in *Proceedings of the 58th IEEE Conference on Decision and Control*, 2019.

[38] H. K. Khalil, *Nonlinear systems; 3rd ed.* Upper Saddle River, NJ: Prentice-Hall, 2002, the book can be consulted by contacting: PH-AID: Wallet, Lionel. [Online]. Available: <https://cds.cern.ch/record/1173048>

[39] D. Bertsekas, "Necessary and sufficient conditions for a penalty method to be exact," *Mathematical programming*, vol. 9, pp. 87–99, 1975.

[40] X. Chen, Z. Lu, and T. K. Pong, "Penalty methods for a class of non-lipschitz optimization problems," *SIAM Journal on Optimization*, vol. 26, no. 3, pp. 1465–1492, 2016.

[41] G. Di Pillo, *Exact Penalty Methods*. Dordrecht: Springer Netherlands, 1994, pp. 209–253.

[42] M. H. Cohen and C. Belta, "Approximate optimal control for safety-critical systems with control barrier functions," in *2020 59th IEEE conference on decision and control*. IEEE, 2020, pp. 2062–2067.

[43] M. Bergounioux and K. Kunisch, "Augmented lagrangian techniques for elliptic state constrained optimal control problems," *SIAM Journal on Control and Optimization*, vol. 35, no. 5, pp. 1524–1543, 1997.

[44] L. S. Pontryagin and V. G. Boltyanskii, "Rv gamkrelidze a ef mishchenko. the mathematical theory of optimal processes," *Interscience, New York*, vol. 171, pp. 276–294, 1962.

[45] J. Logsdon and L. Biegler, "Decomposition strategies for large-scale dynamic optimization problems," *Chemical Engineering Science*, vol. 47, pp. 851–864, 1992.

[46] M. Laroussi, S. Bekeschus, M. Keidar, A. Bogaerts, A. Fridman, X. Lu, K. Ostrikov, M. Hori, K. Stapelmann, V. Miller *et al.*, "Low-temperature plasma for biology, hygiene, and medicine: Perspective and roadmap," *IEEE Transactions on Radiation and Plasma Medical Sciences*, vol. 6, no. 2, pp. 127–157, 2021.

[47] A. D. Bonzanini, K. Shao, A. Stancampiano, D. B. Graves, and A. Mesbah, "Perspectives on machine learning-assisted plasma medicine: Toward automated plasma treatment," *IEEE Transactions on Radiation and Plasma Medical Sciences*, vol. 6, no. 1, pp. 16–32, 2021.

[48] D. Rodrigues, K. J. Chan, and A. Mesbah, "Data-driven adaptive optimal control under model uncertainty: An application to cold atmospheric plasmas," *IEEE Transactions on Control Systems Technology*, vol. 31, pp. 55–69, 2023.